^{208}Pb(d,p) and (d,t) Reactions with 15- to 25-MeV Deuterons*

G. MUEHLLEHNER, A. S. POLTORAK,† AND W. C. PARKINSON
Cyclotron Laboratory, Department of Physics, The University of Michigan, Ann Arbor, Michigan

AND

R. H. BASSEL
Oak Ridge National Laboratory, Oak Ridge, Tennessee
and
Brookhaven National Laboratory, Upton, New York

(Received 28 December 1966)

The differential cross sections for the single-particle states of ^{209}Pb and single-hole states of ^{207}Pb excited in the ^{208}Pb(d,p) and ^{208}Pb(d,t) reactions, respectively, have been measured using deuterons of energies 14.8, 20.1, and 24.8 MeV and the distorted-wave-approximation parameters for fitting the data determined. As a result, it is now possible to determine l values with confidence and to extract spectroscopic factors with a reliability of about 30% from data for high-A nuclei in this range of deuteron energies.

I. INTRODUCTION

THE new generation of sector-focused cyclotrons and the larger tandem Van de Graaffs together with their ancillary apparatus for high-resolution charge-particle spectroscopy permit for the first time the investigation of individual states of heavy nuclei at energies well above the Coulomb barrier. In the analysis of differential cross sections from direct reactions the distorted-wave approximation (DWA) continues to be most useful for the extraction of spectroscopic information. However, it is relatively untested in the region of high-mass nuclei at incident-deuteron energies well above the Coulomb barrier. The "doubly magic" nucleus ^{208}Pb provides a convenient test case. Presumably the low-lying levels of ^{209}Pb are "pure" single-particle states, while those of the ^{207}Pb are "pure" hole states. Spins and parities of these states are presumably known and spectroscopic factors should be close to unity for the stripping reactions and $(2J+1)$ for the pickup reactions. Thus predictions of the shapes and magnitudes of the differential cross sections provide an important test of the theory.

A complete program for such a study implies knowledge of the scattering wave functions in both entrance and exit channels as well as the transfer angular distributions. To implement this we have measured absolute differential cross sections for seven levels in ^{209}Pb and six levels in ^{207}Pb, for incident deuteron energies of 14.8, 20.1, and 24.8 MeV. At the same time deuteron elastic angular distributions were measured. For the exit channels, data for proton scattering in the Pb region is sparse and that for triton scattering nonexistent. Thus, we are forced to rely on optical-model parameters extrapolated in energy and from other mass regions.

* Supported in part by the U. S. Atomic Energy Commission.
† Present address: Conductron Corporation, Ann Arbor, Michigan.

II. EXPERIMENTAL

Deuterons from The University of Michigan 83-in. sector-focused cyclotron[1] were used to bombard self-supporting targets of the order of 2 mg/cm^2 thickness of lead enriched[2] to 99.3% in ^{208}Pb. The reaction products, protons, tritons and elastically scattered deuterons, were analyzed in energy with the first of three spectrometer magnets[1] and were recorded both in nuclear emulsions and with a sonic spark chamber. The nuclear track plates used at the image surface of the magnet were Ilford type K-2 with 100-μ emulsions. The sonic spark chamber is similar in mechanical design to that developed at the University of Rochester.[3] It consists of two sections, a proportional counter and a spark gap. The signal from the proportional counter permits particle identification, and at the same time, is used to apply the high voltage to the spark gap. The sonic waves from the spark are detected by a transducer located at one end of the chamber. The time difference between the proportional counter signal and the signal from the transducer is converted to a voltage pulse by a time–to–pulse-height converter. The output pulses of the converter, the height of which is proportional to the distance from the transducer to the point at which the particle crossed the gap, are analyzed in height in a multichannel analyzer.

The thickness of each target was determined by measusing the energy loss of 5.48-MeV α particles from ^{241}Am passing through them using a calibrated silicon surface-barrier detector and pulse-height analyzer. To verify experimentally the relation between the thickness and the energy loss, the thickness of several natural lead films was determined by weighing small portions of known area on a microbalance. The measured energy

[1] W. C. Parkinson, R. S. Tickle, P. T. J. Bruinsma, J. Bardwick, and R. Lambert, Nucl. Instr. Methods **18/19**, 92 (1962).
[2] The enriched ^{208}Pb was obtained in metal form from Oak Ridge National Laboratory.
[3] H. W. Fulbright, J. A. Robbins, and A. K. Hamann, University of Rochester Report NYO-10261 (unpublished).

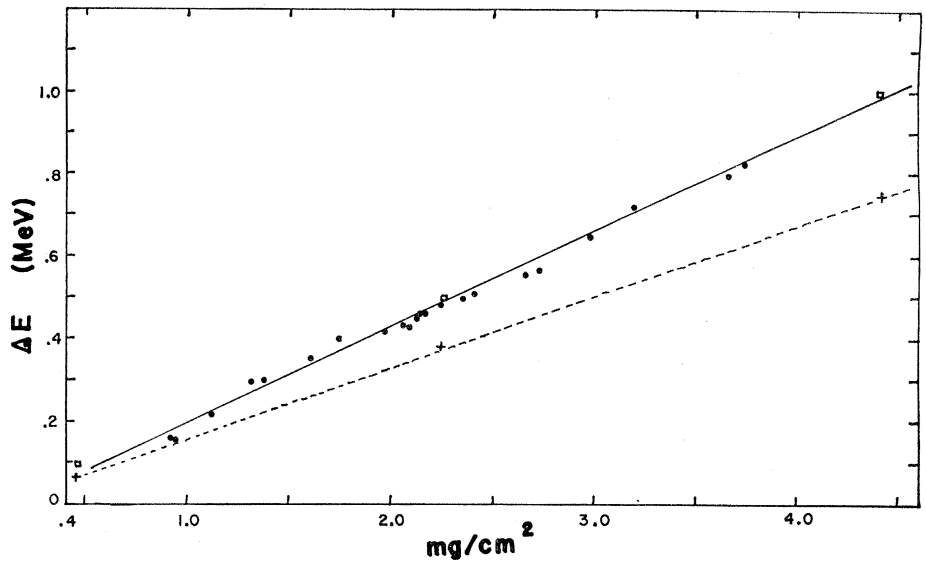

FIG. 1. Energy loss of 5.48-MeV α particles in lead foils. Solid circle: data; open square: Aron, Hoffman, and Williams; plus sign: Williams and Boujot.

loss as a function of target thickness is shown in Fig. 1 together with the calculated loss.[4] It is interesting to note that the measured results are in much better agreement with the calculations of Aron, Hoffman, and Williams, than with Williamson and Boujot. The uncertainty in the target thickness is estimated as less than 10%.

The intensity of the deuteron beam on the target was measured by means of a Faraday cup and current integrator. At scattering angles less than 10°, where the Faraday cup interfered with the scattered particles, a silicon surface barrier detector mounted at 45° and calibrated against the current integrator was used. The absolute solid angle of the reaction products magnet and the differential solid angle across the image surface has been determined, and it is known to approximately 5%. As a result, the uncertainty in the measured absolute differential cross section is estimated to be less than 15%.

The energy of the deuteron beam on the target is determined by the second beam preparation magnet and the slits associated with it.[1] The field at one point in the magnet gap is measured with a nuclear magnetic resonance device, and this has been related to the particle momentum by measuring the resonance at[5] $E_{p\,(\mathrm{lab})}=14.233\pm0.010$ MeV in $^{12}C(p,p)$. While as yet there has been no direct calibration at higher energies, because of the conservative design of the magnet, the integrated magnetic field is believed to track linearly with the NMR frequency.

[4] W. A. Aron, B. G. Hoffman, and F. C. Williams, Radiation Laboratory, University of California, Berkeley, Report AECU-663, 1951 (unpublished); C. Williamson and J. P. Boujot, Saclay report, 1962 (unpublished).

[5] E. Adelberger and C. A. Barnes, Bull. Am. Phys. Soc. **10**, 1195 (1965); J. Cerny, R. Pehl, G. Butler, D. Flemina, C. Maples, and C. Detrae, Phys. Letters **20**, 35 (1966).

III. RESULTS

A. Deuteron Elastic Scattering

The measured angular distributions for the elastic scattering of deuterons at the three energies 14.8, 20.1, and 24.8 MeV are shown in Fig. 2 together with the predictions of the optical model. One set of parameters determined from elastic scattering at[6] 21.6 MeV was used in the calculations for all three energies. These are listed in Table III.

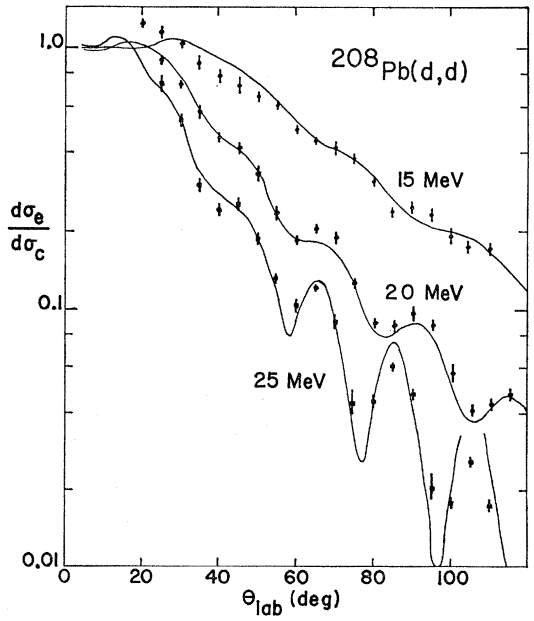

FIG. 2. Angular distributions of elastically scattered deuterons. The points are experimental data; the lines, optical-model predictions. (g.s.≡ground state.)

[6] J. L. Yntema, Phys. Rev. **113**, 261 (1959).

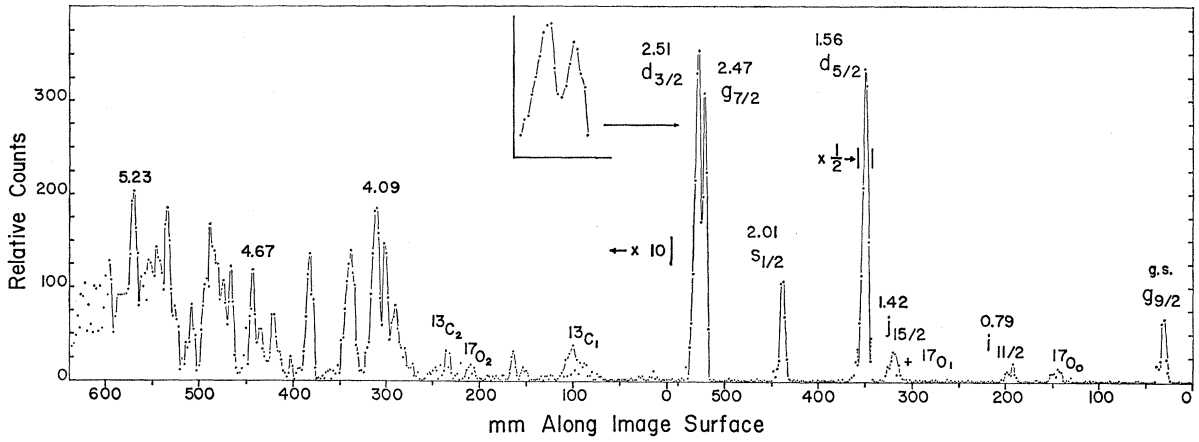

FIG. 3. Typical spectrum obtained in the reaction ^{208}Pb(d,p)^{209}Pb, at a deuteron energy of 20.1 MeV. $\theta=35°$.

B. The (d,p) Reaction

A typical spectrum obtained on nuclear emulsions for the ^{208}Pb(d,p)^{209}Pb reaction is shown in Fig. 3 for the incident deuteron energy of 20.1 MeV. Proton groups corresponding to the single-particle levels are identified on the figure together with the excitation energies. The Q values of the ground state and the excitation energies as determined in these measurements are given in Table I. The two levels at 2.47-MeV excitation are shown in the inset of Fig. 3. The separation of 40±3 keV was determined from the known dispersions of the magnetic analysis system. While no attempt was made to study the levels observed above an excitation of 3 MeV, they presumably arise from core excitation and higher-order processes.

The angular distributions of the proton groups for these seven levels are shown in Fig. 4 for the three incident deuteron energies. These measurements were made using both nuclear emulsions and the sonic spark chamber. The solid curves are the results of the fit to the data by DWA analysis (see Sec. IV).

C. The (d,t) Reaction

A typical spectrum obtained both on nuclear emulsions and with the sonic spark chamber for the ^{208}Pb-(d,t)^{207}Pb reaction at an incident deuteron energy of 24.8 MeV is shown in Fig. 5. The spark-chamber spectrum was plotted directly from the multichannel analyzer using an x-y plotter. The group at the left in the spark chamber spectrum results from a "start" pulse from the proportional counter without a corresponding "stop" pulse from the spark chamber, while the group at the right is due to noise in the electronic system. The spatial resolution of the spark chamber is approximately 7 mm. This relatively poor resolution results in part from the finite thickness of the chamber (~3 mm) and the fact that the image surface of the analyzer magnet makes an angle of approximately 40° with the ion-optic axis. The six single-hole states are identified on the figure, together with their excitation energies. Three weak levels (maximum differential cross section ≤10 μb/sr) in the vicinity of the $h_{9/2}$ have not been studied. The Q value of the ground state and the excitation energies as determined in these measurements are compared with previous results in Table II.

The angular distributions of the triton groups corresponding to the six single-hole levels are shown in Fig. 6 for the three incident-deuteron energies, together with the fit to the data by DWA analysis (see Sec. IV). In

TABLE I. Comparison of Q values and excitation energies (in MeV) for ^{208}Pb(d,p)^{209}Pb.

Level	Present work	Mukherjee[a]	Erskine[b]	NDS[c]
$g_{9/2}$	$Q=1.70\pm0.01$	1.6	1.705±0.015	···
$i_{11/2}$	$E_x=0.79$	0.77	0.774	0.79
$j_{15/2}$	1.42	1.41	···	1.41
$d_{5/2}$	1.56	1.56	1.563	1.56
$s_{1/2}$	2.01	2.03	2.015	2.03
$g_{7/2}$	2.47	2.47	2.483	2.47
$d_{3/2}$	2.51	2.52	2.527	2.54

[a] P. Mukherjee and B. L. Cohen, Phys. Rev. **127**, 1284 (1962).
[b] J. R. Erskine and W. W. Buechner, Bull. Am. Phys. Soc. **7**, 360 (1962).
[c] *Nuclear Data Sheets*, compiled by K. Way *et al.* (Printing and Publishing Office, National Acadamy of Sciences—National Research Council, Washington 25, D. C.) NRC 5-3-93 to 5-3-94.

TABLE II. Comparison of Q-values and excitation energies (in MeV) for ^{208}Pb(d,t)^{207}Pb.

Level	Present work	Brady[a]	Cohen[b]	Harvey[c]
$p_{1/2}$	$Q=-1.13\pm0.01$		−1.12	−1.10
$f_{5/2}$	$E_x=0.57$	0.570	0.57	0.61
$p_{3/2}$	0.89	0.897	0.90	0.95
$i_{13/2}$	1.64	1.633	1.64	1.61
$f_{7/2}$	2.34	2.339	2.35	2.33
	3.23			
	3.33		3.38	
$h_{9/2}$	3.43		3.47	
	3.59			

[a] F. P. Brady, N. F. Peek, and R. A. Warner, University of California, Davis, Report CNL-UCD 23 (unpublished).
[b] B. L. Cohen, S. Mayo, and R. E. Price, Nucl. Phys. **20**, 360 (1960).
[c] J. A. Harvey, Can. J. Phys. **31**, 278 (1953).

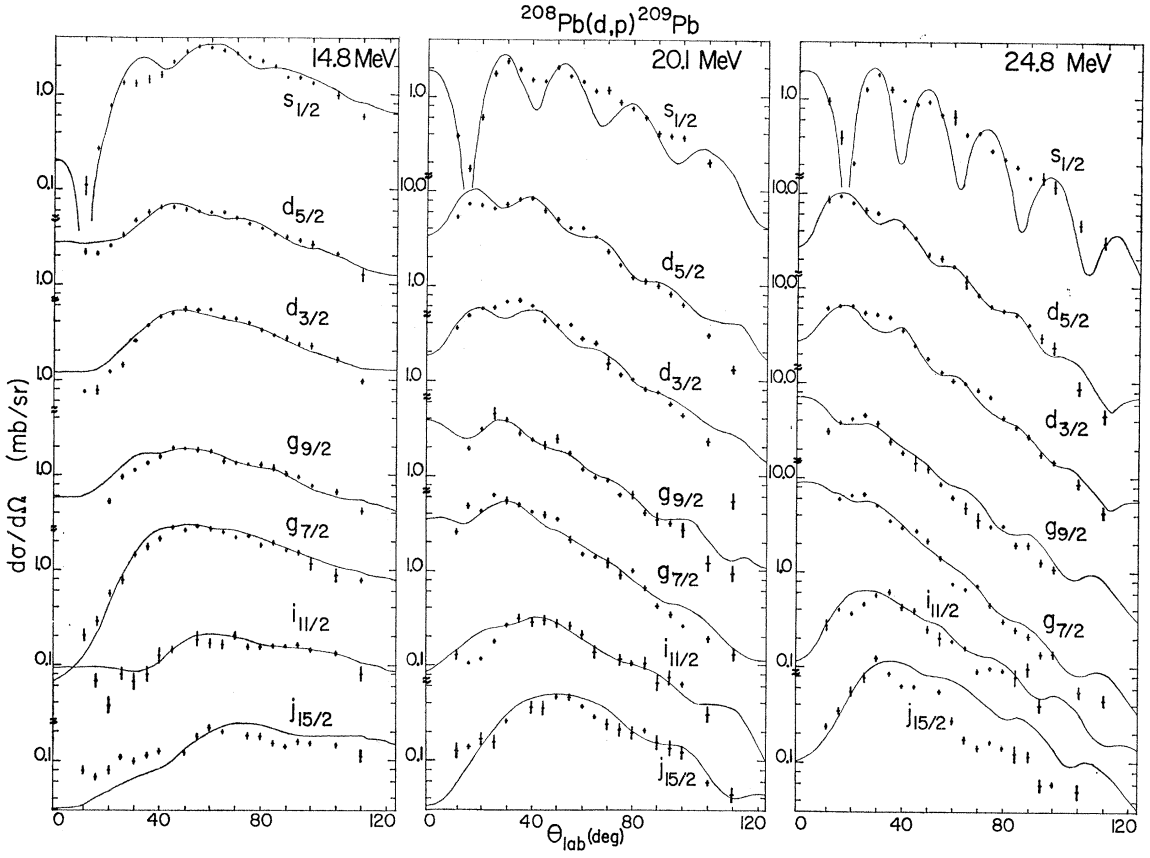

FIG. 4. Angular distributions of protons from the ^{208}Pb$(d,p)^{209}$Pb reactions.

comparing the corresponding distributions at the three energies, the influence of the Coulomb barrier is evident.

IV. THE DWA ANALYSIS

The theory on which this analysis is based is discussed in detail in the papers of Satchler,[7] Lee *et al.*,[8] and references therein. Here we briefly recapitulate the approximations used in our study.

In the transition amplitude for the reaction $A(a,b)B$

$$T=J\int\int X_f^{(-)}(\mathbf{r}_f,\mathbf{k}_f)\langle B,b|V|A,a\rangle \times X_i^{(+)}(\mathbf{r}_d,\mathbf{k}_d)d\mathbf{r}_f d\mathbf{r}_d \quad (1)$$

where the wave functions are taken as solutions of the optical potentials which satisfy elastic scattering in entrance and exit channels.

The effective interaction in the nuclear matrix element is, as usual, taken to be the interaction between the transferred neutron and outgoing projectile.

With the assumption above, the matrix element $\langle B,b|V|A,a\rangle$ factors into a product $\langle B|A\rangle\langle b|V|a\rangle$. The overlap of initial and final target states implies a spectroscopic factor S and a neutron form factor (usually taken as an eigenfunction of a Woods-Saxon well). The matrix element of the effective interaction between wave functions of initial and final projectiles yields a normalization and a range function.

$$D(r)=D_0 f(r).$$

The approximation in which $f(r)$ is taken as a delta function is usually called the zero-range approximation.

If the Hulthén wave function is taken to represent the internal motion of the deuteron, the cross section for the (d,p) reaction is

$$\frac{d\sigma}{d\Omega}=1.5\left(\frac{2J_B+1}{2J_A+1}\right)S_{lj}\sigma_{lsj}(\theta),$$

where σ_{lsj} is a reduced cross section (computed with the code JULIE)[9] for stripping with orbital angular-momentum transfer l, spin transfer s, total angular-momentum transfer j, and J_A and J_B are the spins of the initial and final nuclei. For the (d,t) reaction, assuming an Irving-Gunn wave function for the triton

[7] G. R. Satchler, Nucl. Phys. **55**, 1 (1964).
[8] L. L. Lee, Jr., J. P. Schiffer, B. Zeidman, G. R. Satchler, R. M. Drisko, and R. H. Bassel, Phys. Rev. **136**, B971 (1964).
[9] R. M. Drisko (unpublished).

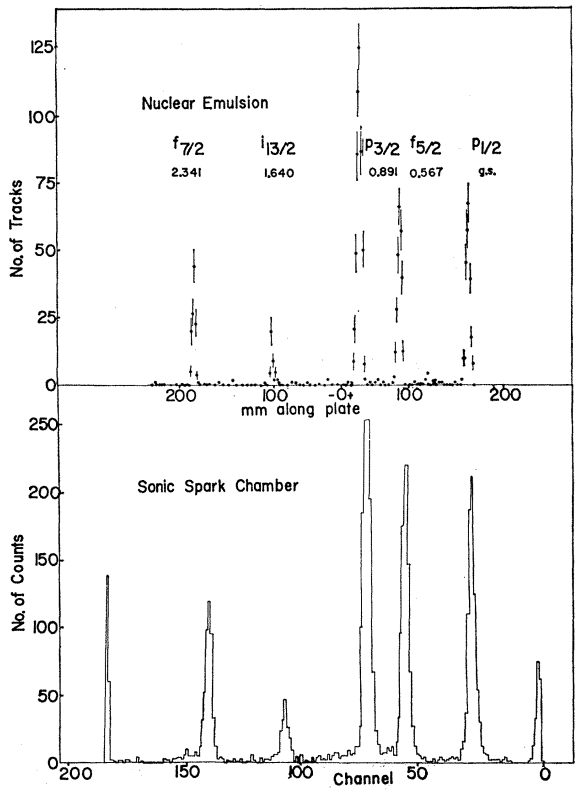

FIG. 5. Typical spectra obtained in the reaction ^{208}Pb(d,t)^{207}Pb at a deuteron energy of 24.8 MeV. $\theta=30°$.

and a Hulthén wave function for the deuteron, the cross section is written[10]

$$d\sigma/d\Omega=3.3S_{lj}\sigma_{lsj}(\theta).$$

In principle, the radial integrals in the matrix element should be carried from the origin to infinity. In practice, it has often been found that better results are obtained, in zero-range approximation, if a nonzero lower limit is used (cutoff radius). Such was indeed found to be the case for the (d,p) reactions. Since the concept of a sharp cutoff is unphysical and arbitrary, corrections to the theory by allowing the range of interaction to be finite and the potentials to be nonlocal were studied in local-energy approximation.[11] These corrections have been shown to reduce contributions to the matrix element from the interior and thus provide a natural cutoff. In the (d,t) reaction, because of the strong absorption for tritons, the DWA predictions are insensitive to the choice of a cutoff radius. For this reason and since our choice of triton parameters was not based on measurements, studies of finite range and nonlocal corrections seemed superfluous. Instead, it was decided to concentrate on studying the effect of varying parameters of the triton and neutron wells.

The general form of the optical potentials used was

$$U(r)=U_c(r)-V_0(1+e^x)^{-1}-iW_0(1+e^{x'})^{-1}+4iW_d\frac{d}{dx'}(1+e^{x'})^{-1}$$

where $x=(r-r_0A^{1/3})/a$, $x'=(r-r_0'A^{1/3})/a'$, and $U_c(r)$ is the Coulomb potential for a point charge incident on a uniformly charged sphere of radius $R_c=r_cA^{1/3}$. Since the computer code could not include spin-orbit coupling for large l transfers, its effect in the scattered channels was ignored throughout. Checks were made for small l transfers and the effects found to be small both on the shape and magnitude of the transfer cross sections.

The neutron well is parametrized,

$$U_n(r)=-V_0\left[1-\frac{\lambda}{ra}\left(\frac{\hbar}{2m_pc}\right)^2(\boldsymbol{\sigma}\cdot\mathbf{l})\frac{d}{dx}\right](1+e^x)^{-1}$$

Here the spin-orbit dependence is known to have large effects on the magnitude of the cross section so it is carried throughout. We take $\lambda=25$, a strength appropriate to both the shell-model and optical potentials.

In both the (d,p) and (d,t) studies the deuteron parameters were obtained from an optical model analysis of deuteron elastic scattering at 21.6 MeV.[6] The neutron parameters are similar to parameters found from proton elastic-scattering optical-model analysis, and to parameters which give a reasonable account of the ^{40}Ca(d,p) reactions.[8] They agree quite well with parameters obtained from a Coulomb distorted-wave analysis of ^{208}Pb(d,p)^{209}Pb data at 6–10 MeV.[12]

In the major part of our (d,p) analysis the proton parameters used were obtained by an analysis[13] of

TABLE III. Parameters used in DWA calculations for ^{208}Pb(d,p).

	Protons	Deuterons	Bound neutron	Protons[a]
V_0 (MeV)	52.0	100.0	b	55.4
r_0 (F)	1.25[c]	1.14	1.20	1.158
a (F)	0.65	0.89	0.65	0.713
W_0 (MeV)	0	0		2.0
W_D (MeV)	7.5	13.8		8.4
r_0' (F)	1.25	1.33		1.314
a' (F)	0.76	0.75		0.761
r_c (F)	1.25	1.30		1.25
V_{so} (MeV)	0	0		0
		$\lambda=25$		

[a] Used for 25.1 MeV only.
[b] Calculated by JULIE to give the binding energy of the neutron.
[c] All radii are given by $R=rA^{1/3}$.

[10] R. H. Bassel, Phys. Rev. **149**, 791 (1966).
[11] P. J. A. Buttle and L. J. B. Goldfarb, Proc. Phys. Soc. (London) **83**, 701 (1964); Gy. Bencze and J. Ziumuny, Phys. Letters **9**, 246 (1964); F. G. Perey and D. Saxon, *ibid.* **10**, 107 (1964).
[12] M. Dost and W. Herring, Phys. Letters **19**, 488 (1965).
[13] F. G. Perey, in Contributed Papers edited by F. E. Throw, Argonne National Laboratory report 1964 (unpublished).

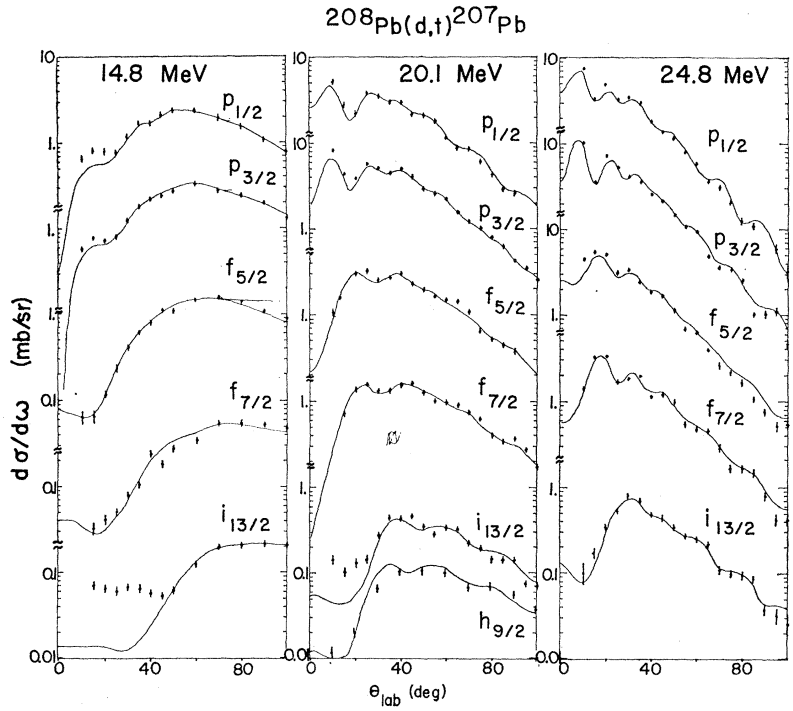

FIG. 6. Angular distributions of tritons from the ^{208}Pb$(d,t)^{207}$Pb transitions.

17-MeV protons scattered from ^{208}Pb. No attempt was made to vary these with energy. The triton parameters were obtained by extrapolation of ^{3}He parameters.[14]

The appropriate numerical values used are listed in Table III for the (d,p) reaction and in Table VIII for the (d,t) reactions.

A. The (d,p) Reaction

Calculations were first made in zero-range approximation with all potentials taken as local. Lower cutoff radii of 0, 6, and 8 F were used in the integration of the transition amplitude. The dependence of the predicted angular distributions on the cutoff radius ranged from being moderately insensitive for orbitals with a large number of nodes (see for example Fig. 7) to very sensitive for orbitals with few nodes (i.e., large l-values) as illustrated in Fig. 8 for the $l=7$ transition at 25.1 MeV. The choice of cutoff which best describes the data, in the sense of both magnitude and shape of the angular distributions, fluctuated with energy and with the l value of the transferred neutron.

Since this situation is both unsatisfying and un-

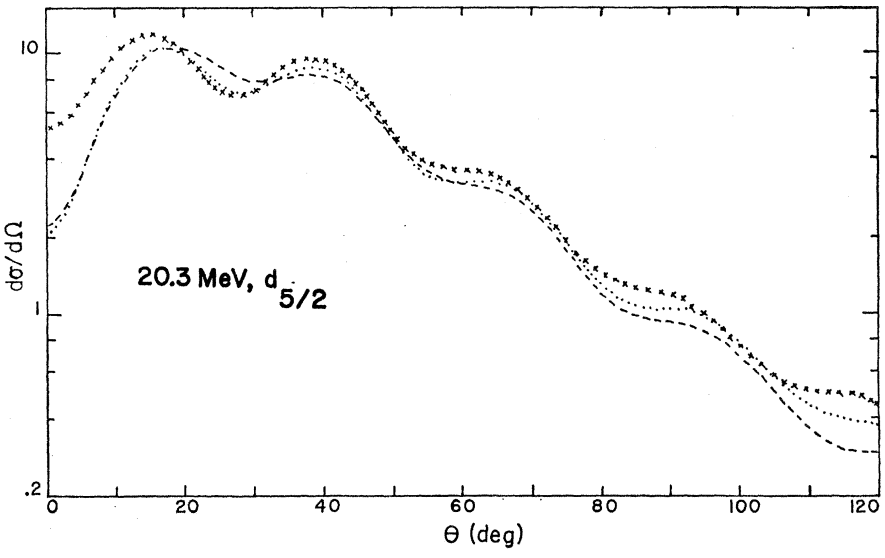

FIG. 7. The effect of the cutoff radius on the distorted-wave predictions for the transition to the $d_{5/2}$ level. Zero range: crosses—lower cutoff = 0 F; dotted line—lower cutoff = 6 F; dashed line—lower cutoff = 8 F.

[14] R. H. Bassel (to be published).

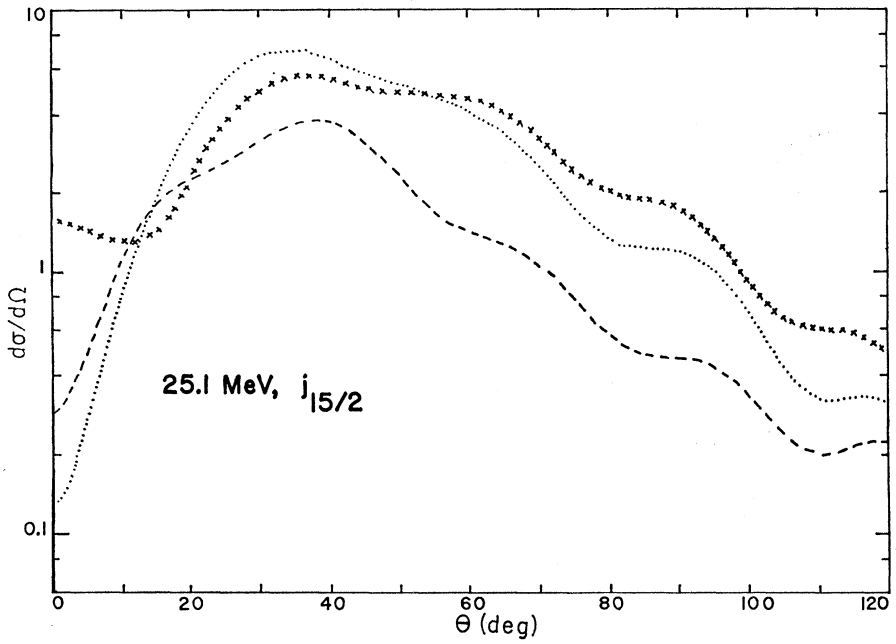

FIG. 8. The effect of the cutoff in distorted-wave predictions for the transition to the $d_{15/2}$ level. Zero range: crosses—lower cutoff=0 F; dotted line—lower cutoff=6 F; dashed line—lower cutoff=8 F.

reliable, the computations were then extended to include a finite-range neutron-proton interaction and nonlocal potentials, using the local-energy approximation (LEA) for both corrections.

For the finite-range modification this consists of introducing a radial factor

$$\Lambda(r)=1-Y(r),$$

$$Y(r)=\frac{[U_d(r)-U_p(r)-U_n(r)-B_d]}{4(\hbar^2/mR^2)}. \quad (2)$$

Here U_d, U_p, and U_n are the potentials for the deuteron, proton, and bound neutron, B_d is the separation energy of the deuteron, R is the range of the force, and m is the atomic mass unit.

This correction has been shown to accurately reproduce the exact finite-range correction provided $U_d=U_p+U_n$.[15]

The nonlocal corrections in LEA are included in similar fashion with factors

$$F_i(r)=\frac{C}{[1-(\mu_i\beta_i^2/2\hbar^2)U_i]^{1/2}}, \quad (3)$$

where i refers to particle, μ_i is the reduced mass, β_i is the nonlocality range, and C is a constant equal to unity for scattered functions and greater than one for bound orbitals in order to satisfy the normalization condition.

For positive energy this correction reproduces, to good approximation, the reduction of the wave function in the interior, (the Perey effect)[16] caused by the nonlocality of the potential. For bound orbitals it is not yet known whether a local potential, with parameters deduced from scattering, in combination with the nonlocal correction factor can adequately represent an eigenfunction of a nonlocal potential. A further uncertainty is the character of the nonlocality for particles near the top of the Fermi sea. For this energy region there is evidence that the ratio of effective mass to mass is of order unity or greater.[17] Thus, the correction implied by Eq. (3) may be incorrect in detail.

Accordingly, two sets of calculations were performed: One in which all wave functions are corrected for nonlocality, and a second set in which this correction is applied only to scattered waves. Again the same set of cutoff radii were used.

In these calculations the range R is taken as 1.25 F.[18] The nonlocality ranges used were $\beta_d=0.54$ F and $\beta_{\text{nucleon}}=0.85$ F, which values are obtained if the energy dependence of the optical potential is assumed to be due entirely to nonlocality.

Typical, but not universal, effects due to these corrections are shown in Fig. 9, where it is seen that the finite range and nonlocal corrections to the distorted waves suppress the magnitude of the cross section but make little alteration in the shape. Applying the LEA to the bound orbital enhances the tail of this

[15] J. K. Dickens, R. M. Drisko, F. G. Perey, and G. R. Satchler, Phys. Letters **15**, 337 (1965).

[16] F. G. Perey, in *Direct Interactions and Nuclear Reaction Mechanisms* edited by E. Clemtentel and C. Villi (Gordon and Breach Science Publishers, Inc., New York, 1963), p. 125; N. Austern, Phys. Rev. **137**, B752 (1965).

[17] G. E. Brown, J. H. Gunn, and P. Gould, Nucl. Phys. **46**, 598 (1963); G. R. Satchler (private communication).

[18] R. M. Drisko and G. R. Satchler, Phys. Letters **9**, 342 (1964).

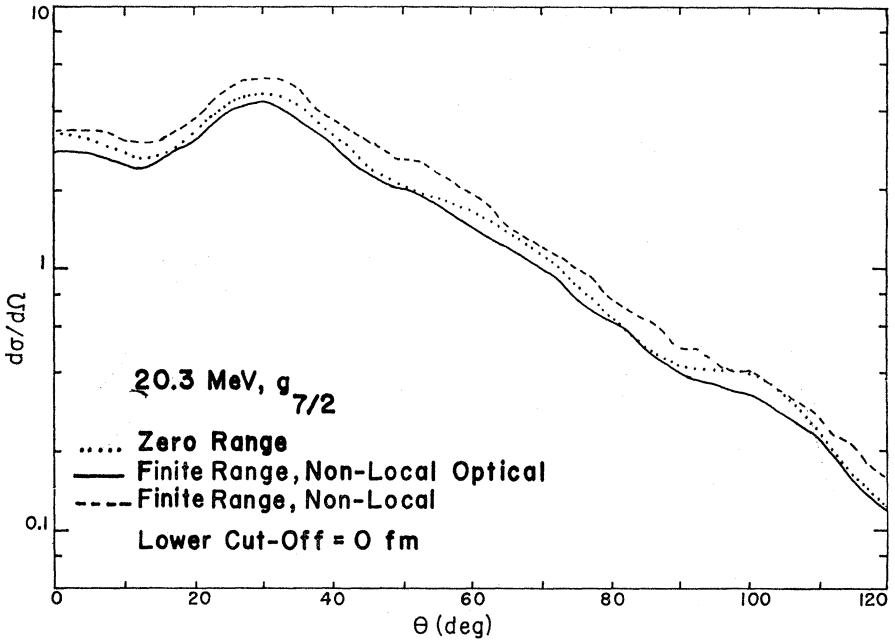

FIG. 9. Typical effects of finite range and nonlocality on the distorted-wave predictions for stripping. Dotted line: zero range; solid line: finite range, nonlocal optical; dashed line finite range, nonlocal; lower cutoff=0 F. Cross sections are in arbitrary units.

function and results in a large increase in cross section again with minimal change in shape.

Examination of this large collection of calculations revealed, with few exceptions, that the shapes of the predicted angular distributions were almost independent of the variations in the DWA theory. The major changes were in the spectroscopic factors. The most consistent prediction of the magnitude of the differential cross sections for all l-values and energies was obtained using a finite range interaction, nonlocal distorted waves and no radial cutoff in the matrix element. The spectroscopic factors for these conditions are listed in Table IV. In the zero-range local theory, with no lower cutoff, the spectroscopic factors are, in general, 10 to 20% smaller than those listed in Table IV, and in the full finite-range nonlocal theory they are some 20–40% smaller.

The entries in Table IV show some variation with deuteron energy. One possible reason for this is that no provision has been made for the change of optical-model parameters with energy in the proton channel. To study this, calculations were made (in zero-range, local approximation) for the transitions initiated by

TABLE IV. Spectroscopic factors for single-particle states in ^{208}Pb$(d,p)^{209}$Pb.

Level	15.0 MeV	20.3 MeV	25.1 MeV
$g_{9/2}$	0.87	0.77	0.67
$i_{11/2}$	1.17	0.78	0.94
$j_{15/2}$	0.96	0.79	1.13
$d_{5/2}$	0.83	1.05	1.00
$s_{1/2}$	0.80	0.90	0.93
$g_{7/2}$	1.08	1.08	1.17
$d_{3/2}$	0.88	1.07	1.17

TABLE V. Comparison of spectroscopic factors at 25 MeV.

Level	"Best" over-all fit	30-MeV proton parameters
$g_{9/2}$	0.67	0.80
$i_{11/2}$	0.94	1.06
$j_{15/2}$	1.13	1.00
$d_{5/2}$	1.00	1.11
$s_{1/2}$	0.93	1.03
$g_{7/2}$	1.17	1.15
$d_{3/2}$	1.17	1.60

24.8-MeV deuterons using parameters from an analysis of 30-MeV proton scattering from ^{208}Pb.[19] The parameters, listed in Table III, are somewhat different from those found at 17 MeV. Perhaps what is most relevant to the present study is the nature of the imaginary potential, which contains a volume term and is centered at a larger radius. The stripping predictions, using this potential, are very similar in shape to those illustrated in Fig. 4, but the spectroscopic factors for no radial cutoff are, in general, improved (see Table V).

B. The (d,t) Reaction

The parameters for triton scattering from ^{208}Pb are not known. There have been measurements of ^{3}He scattering from ^{208}Pb at 20 MeV,[20] and this data has been analyzed in terms of an optical model,[14] and the parameters found there used as a basis of this study.

The magnitude, but not the shape, of the angular distributions is also quite sensitive to the parameters of

[19] G. R. Satchler, Nucl. Phys. (to be published).
[20] R. W. Klingensmith, H. J. Hausman, and W. D. Ploughe, Phys. Rev. 134, B1220 (1964).

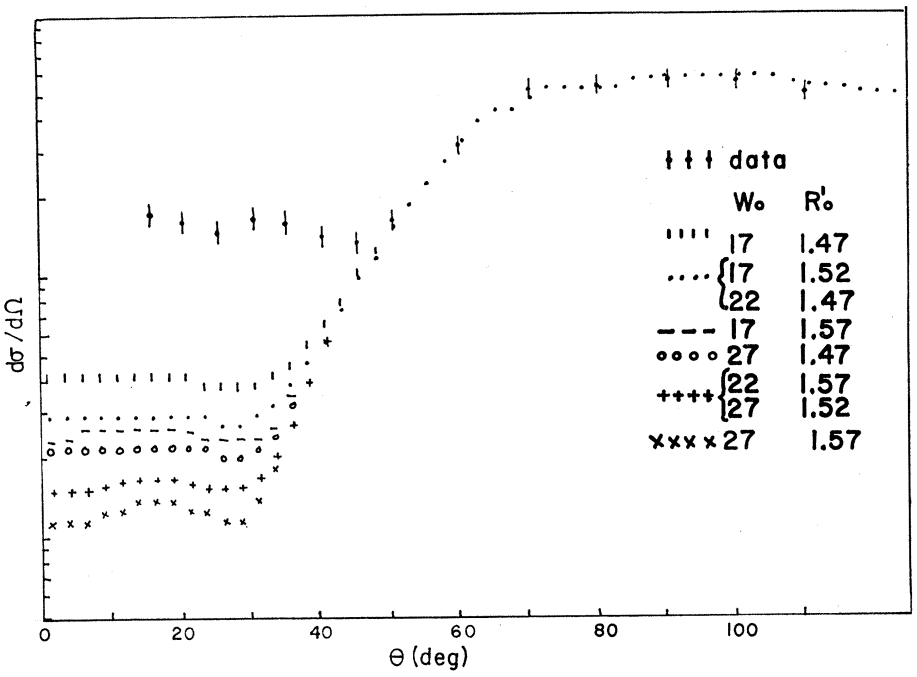

FIG. 10. Effect of triton parameters W_0 and r_0' on shape of distributions for the $i_{13/2}$ transition at 15 MeV. Cross sections are in arbitrary units.

the neutron well. These were determined by arbitrarily deciding to normalize to the $f_{5/2}$ cross section at 25 MeV, holding the triton and deuteron parameters fixed and varying the radius parameter r_0 and diffusivity a of the neutron well. In essence this determines the depth U_n, since the computer is programmed to give the correct separation energy. Acceptable agreement was found with $r_0=1.225$ F and $a=0.7$.

To determine the sensitivity of the differential cross section to these parameters, the radius and diffusivity were changed in small steps around the central values (with compensating changes in the depth U_n). The calculations were made for the $f_{5/2}$ transition at 15 and 25.1 MeV and the results, which are the same for both energies, normalized to the strength at the central values, are summarized in Table VI. While the strength varies, the shape of the angular distribution does not. The changes were found to be independent of the energy of the incoming deuteron thus verifying the surface character of the transition. Reducing either r_0 or a results in a deeper well such that the wave function is shifted to smaller radii. This reduces the overlap with the distorted waves and therefore decreases the predicted cross section.

A change in the strength of the spin-orbit well has no effect on the shape of the distributions. The change in cross section is approximately proportional to $-l$ for $J_>=l+\frac{1}{2}$ transitions and to $(l+1)$ for $J_<=l-\frac{1}{2}$ transitions as is to be expected. However, the effect on magnitude with changes in spin orbit is surprisingly weak especially for orbitals with a large number of nodes.

Since the parameters for tritons may be different from those for ^{3}He ions, we felt at liberty to make small variations in the parameters about the ^{3}He values in order to assess their importance and to optimize agreement with the data. It was found that the cross sections, both shape and magnitude, were insensitive to variation in the real well for tritons, but that the magnitude was quite sensitive to changes in the imaginary well, as summarized in Table VII for the 15-MeV case. With the exception of the $i_{13/2}$ transition, as shown in Fig. 10, the change in shape of the angular distribution with variation of the triton parameters was small.

Two criteria were used in selecting the "best" triton parameters (Table VIII). These were the quality of fit to the shape of the $i_{13/2}$ angular distribution at forward angles and optimizing the magnitude of the calculated cross section at all three energies. To obtain approxi-

TABLE VI. Variation of differential cross section of the $f_{5/2}$ level with neutron parameters r_0 and a. The value for $r_0=1.225$ and $a=0.70$ was arbitrarily set to unity.

r_0 \ a	0.65	0.70	0.75
1.200	0.75	0.85	0.95
1.225	0.89	1	1.13
1.250	1.06	1.19	1.34

TABLE VII. Variation of differential cross section with triton parameters W_0 and r_0' at $E_d=15$ MeV. The value for $r_0'=1.52$ and $W_0=22$ was arbitrarily set to unity.

r_0' \ W_0	17	22	27
1.47	1.33	1.20	1.09
1.52	1.13	1	0.89
1.57	0.93	0.81	0.71

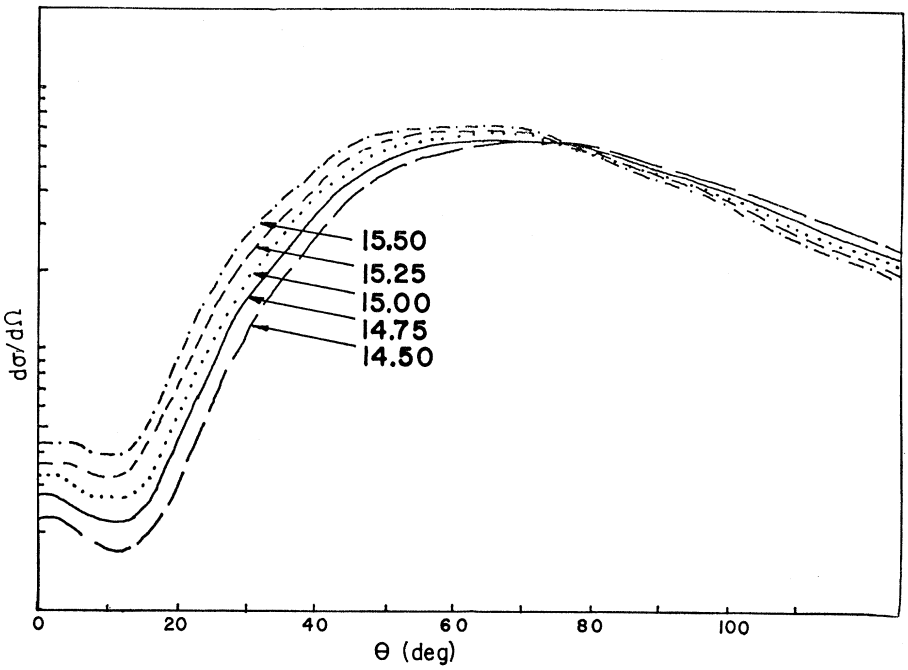

FIG. 11. Predicted dependence of (d,t) cross section to the $f_{5/2}$ level on energy at 15 MeV. Cross sections are in arbitrary units.

mately the same spectroscopic factors at all three energies it was necessary to vary the depth of the imaginary well from 17 MeV at the lowest deuteron energy to 22 MeV at $E_d=25.1$ MeV. This was the only energy dependence found. This variation of W_0 with energy is somewhat larger than that found for the ^{3}He optical potential for lighter nuclei.[21] However, using the median energy parameters at all three energies results in only a 6% decrease in spectroscopic factors at 15.1 MeV and an increase of about 8% at 25.1 MeV.

The spectroscopic factors are listed in Table IX. Note that, in general, those for $J_<$ are larger than expected, while for $J_>$ they are smaller. To a lesser extent the same is true for the spectroscopic factors found in the (d,p) reactions.

At low-incident-deuteron energies there may be considerable uncertainty in spectroscopic factors if the energy is not precisely known. This is illustrated in Fig. 11. At higher energies this sensitivity to energy is much smaller as seen in Fig. 12.

TABLE VIII. Parameters used in DWA calculations for ^{208}Pb(d,t).

Deuteron	Neutron	Triton
$V_0=100$ MeV		168 MeV
$W_0=0$		(see below)[a]
$r_0=1.14$ F	1.225 F	1.14 F
$r_c=1.3$ F		1.4 F
$a=0.89$ F	0.70 F	0.723 F
$r_0'=1.33$ F		1.52 F
$a'=0.75$ F		0.77 F
$W_D=13.8$ MeV		0
	$\lambda=25$	

[a] For the triton: $W_0=17$ MeV for $E_d=15$ MeV, $W_0=19$ MeV for $E_d=20.3$ MeV, and $W_0=22$ MeV for $E_d=25.1$ MeV.

TABLE IX. Spectroscopic factors[a] for single-hole states in ^{208}Pb$(d,t)^{207}$Pb.

Level	14.8 MeV	20.1 MeV	24.8 MeV
$p_{1/2}$	2.18	2.12	2.12
$f_{5/2}$	6.60	7.20	6.00
$p_{3/2}$	3.76	3.80	3.32
$i_{13/2}$	14.00	13.02	14.00
$f_{7/2}$	6.08	6.40	5.76
$h_{9/2}$		10.00	

[a] Spectroscopic factors given by the DWA analysis using the parameters of Table VIII.

V. DISCUSSION

The preceding paragraphs have described a study of the applicability of the distorted wave theory for single-nucleon transfer reactions on ^{208}Pb. In particular, the use of parameters available in the literature was emphasized.

The results of the study indicate that using the available parameters the shapes of angular distributions are well given, but there is greater uncertainty in the magnitude. The only major departure in shape was the distribution of the $i_{13/2}$ in the (d,t) reaction at low energies and forward angles.

With respect to the magnitudes, our simple procedure gave spectroscopic factors within 20% for both the (d,p) reactions and the (d,t) reactions. The most glaring exceptions were for the $g_{9/2}$ transition in the (d,p) reaction at 25.1 MeV, and for the $f_{7/2}$ transition in the (d,t) reaction at 15.1 and 25.1 MeV. These variances

[21] E. F. Gibson, B. W. Ridley, J. J. Kraushaar, M. E. Rickey, and R. H. Bassel, Phys. Rev. 155, 1194 (1967).

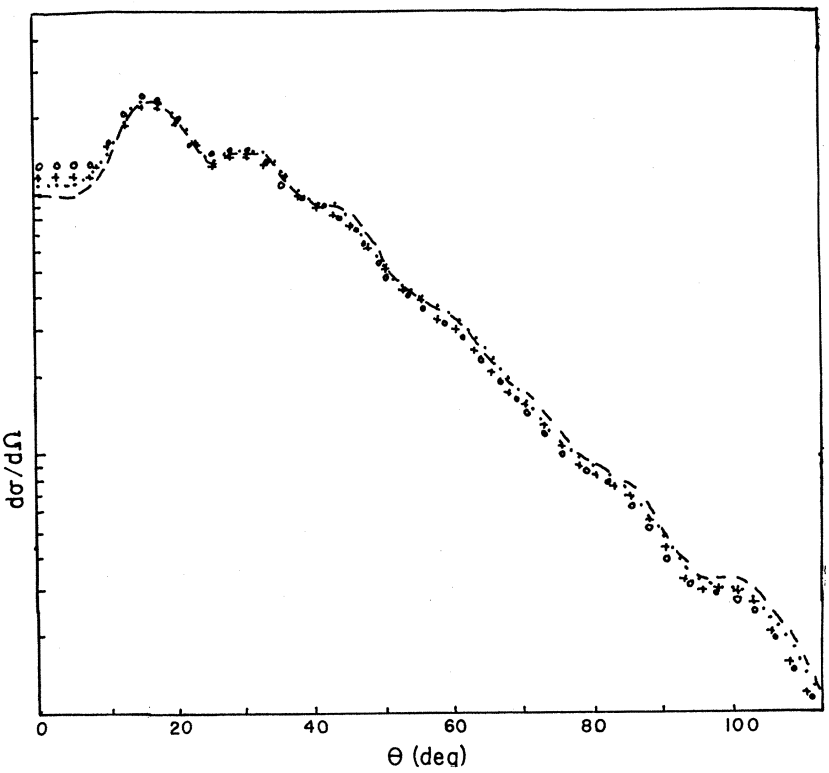

FIG. 12. Predicted dependence of (d,t) cross section to the $f_{5/2}$ level on energy at 25 MeV. Open circles: 25.50; crosses: 25.30; dotted line: 25.00; dashed line: 24.75. Cross sections are in arbitrary units.

are believed due to a spin-orbit effect in the (d,t) reaction and to both spin-orbit effect and uncertainty in the energy dependence of the proton parameters in the (d,p) reactions. Since changing the strength of the spin-orbit potential for the bound orbital improved the agreement by only a few percent, it is possible that the fault lies in the radial shape assumed for this potential—e.g., there is evidence in scattering[22] for a departure from the Thomas form we have used.

Finite-range and nonlocal corrections in the distorted waves yielded important improvements in the theory for (d,p) reactions, especially in predicting the absolute magnitudes. Nonlocal corrections to the bound orbital in local-energy approximation considerably over estimate the cross section, in agreement with previous studies of this correction.[18]

In sum, although there are many effects yet to be understood, we believe the distorted-wave approximation to be a useful tool in the study of high-A nuclei. Orbital-angular-momentum transfers can be assigned with considerable confidence, and spectroscopic factors can, in general, be extracted with uncertainties of less than 30%.

ACKNOWLEDGMENTS

We gratefully acknowledge useful conversations with G. R. Satchler and R. M. Drisko.

[22] L. J. B. Goldfarb, G. W. Greenlees, and M. B. Hooper, Phys. Rev. 144, 829 (1966); L. N. Blumberg, E. E. Gross, A. van der Woude, A. Zucker, and R. H. Bassel, *ibid.* 147, 812 (1966).